

Three centuries of insect outbreaks across the European Alps

Ulf Büntgen¹, David Frank¹, Andrew Liebhold², Derek Johnson³, Marco Carrer⁴, Carlo Urbinati⁵, Michael Grabner⁶, Kurt Nicolussi⁷, Tom Levanic⁸ and Jan Esper¹

¹Swiss Federal Research Institute WSL, Zürcherstrasse 111, 8903 Birmensdorf, Switzerland; ²Northern Research Station, USDA Forest Service, 180 Canfield St, Morgantown, WV 26505, USA; ³University of Louisiana, PO Box 42451, Lafayette, LA 70504, USA; ⁴Università degli Studi di Padova, Dip. TeSAF, Treeline Ecology Research Unit, Agripolis, 35020 Legnaro (PD), Italy; ⁵Università Politecnica delle Marche, SAPROV, Forest Ecology and Management, Via Breccia Bianche, 60131 Ancona, Italy; ⁶BOKU, University of Natural Resources and Applied Life Sciences, Gregor-Mendel-Str. 33, 1180 Vienna, Austria; ⁷Institute for High Mountain Research, Innrain 52, 6020 Innsbruck, Austria; ⁸Slovenian Forestry Institute, Vecna pot 2, 1000 Ljubljana, Slovenia

Summary

Authors for correspondence:

Ulf Büntgen

Tel: +41 44 739 2679

Email: buentgen@wsl.ch

David Frank

Tel: +41 44 739 2282

Email: frank@wsl.ch

Received: 27 November 2008

Accepted: 8 February 2009

New Phytologist (2009) **182**: 929–941

doi: 10.1111/j.1469-8137.2009.02825.x

Key words: climate change, larch budmoth, *Larix decidua*, population ecology, tree rings, *Zeiraphera diniana*.

- Knowledge of the persistence of regular larch budmoth outbreaks is limited in space and time. Although dendrochronological methods have been used to reconstruct insect outbreaks, their presence may be obscured by climatic influences.
- More than 5000 tree-ring series from 70 larch host and 73 spruce nonhost sites within the European Alps and Tatra Mountains were compiled. Site-specific assessment of growth–climate responses and the application of six larch budmoth detection methods considering host, nonhost and instrumental time-series revealed spatiotemporal patterns of insect defoliation across the Alpine arc.
- Annual maps of reconstructed defoliation showed historical persistence of cyclic outbreaks at the site level, recurring *c.* every 8–9 yr. Larch budmoth outbreaks occurred independently of rising temperatures from the Little Ice Age until recent warmth. Although no collapse in outbreak periodicity was recorded at the local scale, synchronized Alpine-wide defoliation has ceased during recent decades.
- Our study demonstrates the persistence of recurring insect outbreaks during AD 1700–2000 and emphasizes that a widely distributed tree-ring network and novel analysis methods can contribute towards an understanding of the changes in outbreak amplitude, synchrony and climate dependence.

Introduction

Regular population oscillations are well known from a variety of animal species, including foliage-feeding Lepidoptera (Myers, 1988; Berryman, 1996; Kendall *et al.*, 1998; Liebhold & Kamata, 2000). These oscillations are thought to arise from trophic interactions. The resulting periodic outbreaks represent pulsed disturbances, which affect ecosystem structure and function at a variety of temporal and spatial scales. In line with observed climate impacts on ecological processes (Stenseth *et al.*, 2002; Parmesan, 2006), formerly stable cycles in some animal populations may experience a dampening coincident with recent climatic warming (Imms *et al.*, 2008). Because of the lack of long records of cyclic population dynamics, and the paucity of even short-duration time-series for species such

as voles, lemmings and forest grouse (Lindström & Hörnfeld, 1994; Steen *et al.*, 1996), the statistical evidence for the persistence or collapse of population cycles remains elusive (Stenseth, 1999). Exceptional in this regard are forest insect outbreaks, leaving distinct fingerprints in the annual growth of tree rings (Schweingruber, 1979).

Periodic oscillations in the abundance of the larch budmoth (LBM) are notorious, both in terms of regularity as well as the copious amounts of data collected on these oscillations during the middle part of the 20th century (Baltensweiler & Rubli, 1999). In areas of susceptible forests, LBM populations characteristically oscillate over densities ranging from 1 to 30 000 larvae per host tree, with outbreaks recurring every 8–9 yr (Baltensweiler *et al.*, 1977). Several mechanisms have been proposed to explain cycles in LBM population dynamics.

These mechanisms include behavioural changes in population quality (Baltensweiler, 1993b), host–pathogen interactions (Anderson & May, 1980), induced host defences (Fischlin & Baltensweiler, 1979) and host–parasitoid interactions (Turchin *et al.*, 2003). Larvae of LBM feed on the foliage of sub-alpine larch, which occurs extensively in a forest belt across the European Alps (Baltensweiler *et al.*, 1977). During outbreaks, trees may be completely defoliated, and this defoliation occurs synchronously over large areas, affecting various forest ecosystem processes, but rarely triggering tree mortality. Defoliation affects tree growth, and fingerprints of cyclic outbreaks, i.e. reduced tree-ring width (TRW) and maximum latewood density (MXD), contain unique long-term information on herbivore population dynamics, and inferred relationships with climate and/or other environmental factors (Esper *et al.*, 2007). Dendroecological research on insect defoliation, mainly caused by the spruce budworm, has experienced much attention in the northern USA, where refined comparison between host and nonhost species (Swetnam *et al.*, 1985; Morin *et al.*, 1993; Swetnam & Lynch, 1993) and advanced time-series analysis (Ryerson *et al.*, 2003) have allowed outbreak dynamics to be reconstructed over the past six centuries (Speer *et al.*, 2001).

In Europe, several studies investigating the long-term dynamics of LBM populations have been based on tree-ring data. Considerable insight has been gained from reconstructions of LBM outbreaks based on TRW chronologies from two sub-alpine valleys in Switzerland (Weber, 1997), the Italian–French border region (Nola *et al.*, 2006) and the French Alps (Rolland *et al.*, 2001); these studies have reported the regular recurrence of outbreaks, with little evidence for changes in cycle period and amplitude over the last few centuries. A unique 1200-yr-long reconstruction of LBM outbreaks at a single site was developed using TRW and MXD from living trees and historic timbers in the Swiss Alps (Esper *et al.*, 2007). Analysis of space–time patterns, however, cannot be characterized on the basis of reconstructions from a single location alone. Moreover, observations of the local scale may be biased by ecological site condition, stand competition, forest history and human impact. Hence, dynamic patterns, such as the synchrony and occurrence of outbreak waves that spread across the Alps (Bjørnstad *et al.*, 2002; Johnson *et al.*, 2004, 2006), can only be understood by reconstructing outbreak histories at many locations.

To overcome the limitations emerging from the local scale, we present here a unique test bed of 70 host and 73 nonhost tree-ring sites distributed across the European Alps and Tatra Mountains, representing approximately 1 million annually resolved measurements, to identify outbreak-induced growth depressions. After assessing the climate response of each site chronology, fingerprints of LBM defoliation were detected via comparison of the host data with nonhost tree-ring and climate surrogates, as well as the use of time-series analysis. This suite of techniques applied to the network allowed the

reconstruction of varying levels of LBM outbreak intensity back to AD 1700 and the assessment of the spatial distribution of these outbreaks across the entire Alpine arc.

Materials and Methods

Host data

Raw measurements of 3151 TRW series from the European larch (*Larix decidua* Mill.) and 150 MXD series from 70 sites across the Alpine arc and Tatra Mountains were compiled (Fig. 1). This network integrates living trees from Italy, France, Switzerland, Austria, Slovenia and Slovakia. Additional historical wood was collected in three sub-alpine valleys in the Swiss Alps (Büntgen *et al.*, 2006a). Individual measurement series were screened for dating errors and de-trended to remove long-term tree age-related growth trends (Fritts, 1976). For the preservation of high-frequency, inter-annual variability, raw time-series were de-trended using cubic smoothing splines with a 50% frequency-response cut-off equal to 20 yr, and indices calculated as ratios from the estimated growth curves (Cook & Peters, 1981). To retain mid-frequency, inter-annual to multi-decadal scale variability, residuals from 300-yr splines were calculated after power transformation (Cook & Peters, 1997). Site chronologies were calculated using a bi-weight robust mean, with the number of samples per year and the cross-correlation coefficient between all measurements being used for variance stabilization (Frank *et al.*, 2007b). A 30-yr moving window inter-series correlation (R_{bar}) and the expressed population signal (EPS) were applied for signal strength assessment (Wigley *et al.*, 1984).

Mean sample replications of the 70 (host) chronologies were 49 and 25 after dividing into TRW (64) and MXD (six) sites. After truncating each site record at a minimum replication of five series, start and end dates of the TRW chronologies were in the ranges AD 951–1911 and 1958–2004. Start and end dates of the MXD chronologies ranged from 1536 to 1899 and 1973 to 2004. The mean period covered by the 64 TRW host chronologies was 401 yr and decreased to 333 yr after truncation. The mean period covered by the six MXD chronologies was 298 yr and decreased to 250 yr after truncation. The majority of data from elevations ≥ 1400 m asl were derived from 54 sites (Fig. 2a). The average elevations of the TRW and MXD sites were 1688 and 1852 m asl, ranging from 500 to 2300 and 1500 to 2130 m asl, respectively. Sufficient site replication, as a compromise with spatial coverage, was obtained for the period 1700–2000, during which the average distance between all sites was ~ 28 km (Fig. 2b). The most recent increase in inter-site distance up to ~ 60 km resulted from a reduction to only 21 sites that were distributed across six countries in the Alps and Tatra Mountains. Based on spatial autocorrelation and principal component analysis (computed over the common 1905–1958 period), the network was divided into five geographical sub-regions (Fig. 1).

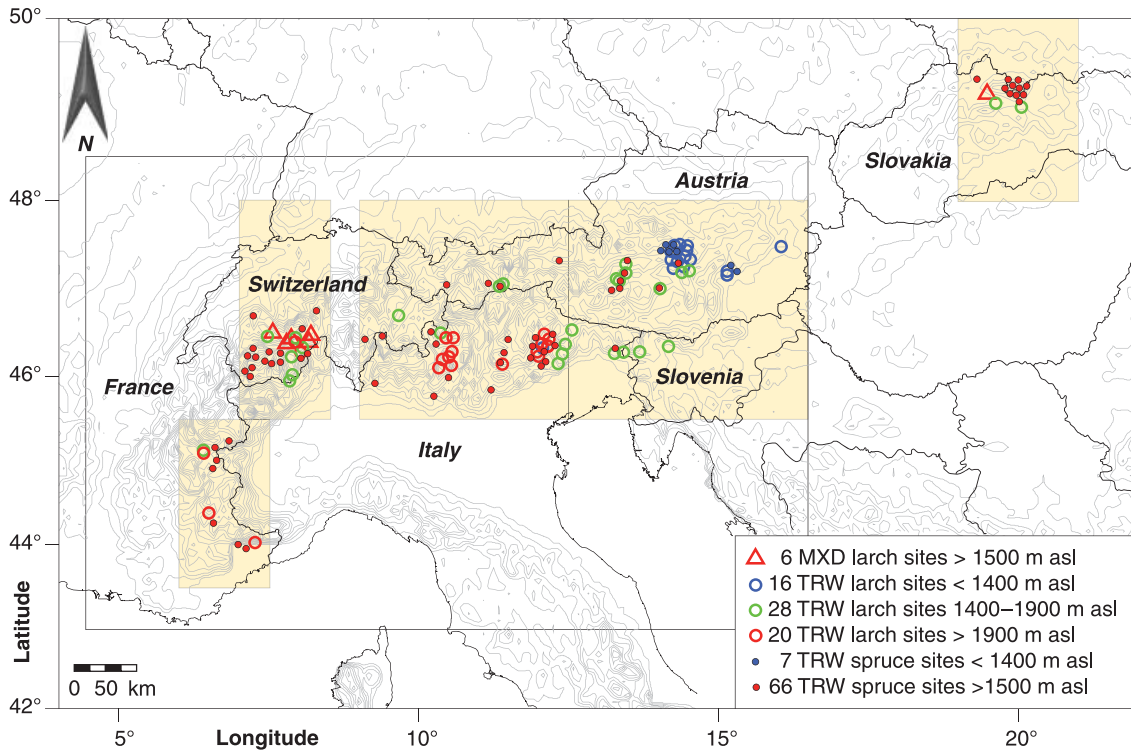


Fig. 1 Location of the host larch and nonhost spruce tree-ring chronologies in the European Alps and Tatra Mountains classified according to elevation (< 1400, 1400–1900, > 1900 m asl) and tree-ring measurements (tree-ring width, TRW; maximum latewood density, MXD). Grey inset frame denotes the greater Alpine region (43.0–48.5°N, 4.0–16.5°E) covered by the 0.5° × 0.5° climate grid (Casty *et al.*, 2005). Shaded insets indicate the five geographical sub-regions used for comparison with the corresponding tree-ring data (Southern Alps, 12 grids, 43.5–45.5°N, 6.0–7.5°E, four host sites; Western Alps, nine grids, 45.5–48.0°N, 7.0–8.5°E, 13 host sites; Central Alps, 35 grids, 45.5–48.0°N, 9.0–12.5°E, 23 host sites; Eastern Alps, 40 grids, 45.5–48.0°N, 12.5–16.5°E, 27 host sites; Tatra, 16 grids, 48.0–50.0°N, 19.0–21.0°E, three host sites).

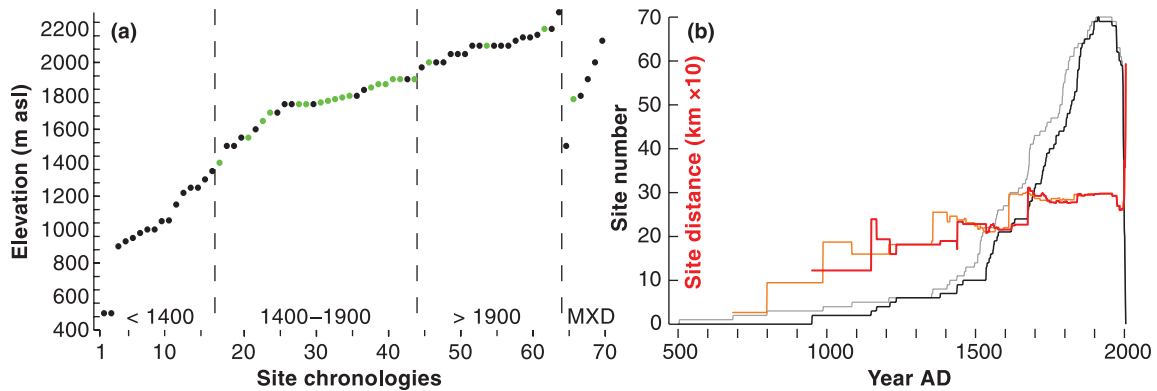


Fig. 2 (a) Distribution of the 70 larch sites relative to elevation (< 1400, 1400–1900, > 1900 m asl) and parameter (tree-ring width, TRW; maximum latewood density, MXD). Green refers to site chronologies from which a distinct –8-yr cycle was detected along the reconstructed larch budmoth (LBM) outbreak time-series (see also Table S1, Supporting Information). (b) Temporal extent of the original (grey) and truncated (less than five series, black) chronologies. Orange (original) and red (truncated, less than five series) curves describe density changes as a function of site-to-site distance.

These comprise four sites in the Southern Alps, 13 sites in the Western Alps, 23 sites in the Central Alps, 27 sites in the Eastern Alps and three sites in the Tatra Mountains. The Eastern Alpine sub-region was additionally split into low and high (< 1400 m asl/> 1400 m asl) elevations.

Site-specific chronology information on location, elevation, attributed geographical sub-region, sample replication, period covered, mean segment length, average growth rate, R_{bar} and EPS statistics, lag-1 autocorrelation, maximum principal component analysis loadings and growth responses to climate is summarized

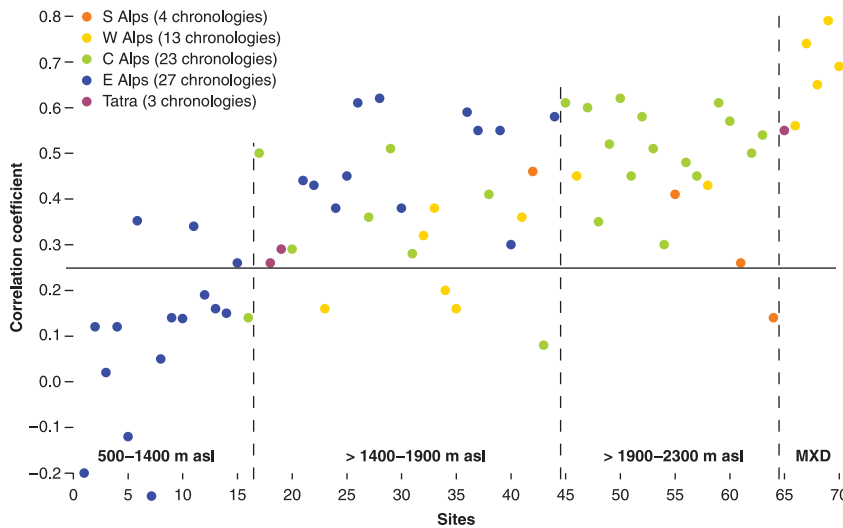


Fig. 3 Maximum correlation with temperature of the host chronologies ordered by elevation and parameter, with colours referring to the five sub-regions. Correlations are computed over 1901–2000 or maximum period of overlap. [See Table S1 (Supporting Information) for details on the individual chronologies.] MXD, maximum latewood density.

in Table S1 (see Supporting Information). Additional information on growth trends and climate sensitivity of the Alpine network is provided in Büntgen *et al.* (2008), whereas details on the Tatra data are given in Büntgen *et al.* (2007).

Because a general understanding of the dominant climatic forcing on annual ring formation at each site would enhance the segregation of climate-induced from insect-induced growth depressions, an in-depth growth–climate response analysis was conducted. High-resolution $0.5^\circ \times 0.5^\circ$ matrices of monthly temperature means and precipitation totals were used (Casty *et al.*, 2005). Although data during the 20th century were exclusively derived from instrumental station readings (CRUTS2.1; Mitchell & Jones, 2005), the importance of monthly resolved documentary evidence increases back in time and helps to extend these records to AD 1659 (Casty *et al.*, 2005). Nevertheless, it should be noted that meteorological station measurements within the greater Alpine region started as early as the mid-18th century (Böhm *et al.*, 2001). Geographical sub-regions, corresponding to those of the tree-ring network, were defined (Fig. 1). Grid boxes for the Tatra region ($48\text{--}50^\circ\text{N}$ and $19\text{--}21^\circ\text{E}$) were directly selected from CRUTS2.1 (freely available at <http://www.cru.uea.ac.uk>). Correlations between the 70 larch chronologies (after 300-yr spline de-trending) and the climatic target data were computed over the 1901–2000 period, using an 18-month window from May of the year before tree growth until October in the current year, plus various seasonal means. Figure 3 summarizes the maximum temperature response of the 70 larch sites. Fifty-two chronologies correlated significantly ($P < 0.01$) with some seasonal mean between April and September (Table S1). Of the 18 remaining records that did not capture a significant climatic signal, 13 were derived from elevations of < 1400 m asl, from which 12 were located in the Eastern Alpine sub-region. All 23 Central Alpine TRW chronologies and those from the Tatra region revealed response optima with a seasonal mean between May and August, whereas a few sites from the

Southern, Western and Eastern sub-regions showed optimum responses to monthly temperature means between April and September. Linkage between site elevation and climate sensitivity was confirmed, as growth at > 1400 m asl was mainly controlled by variations in warm season temperature (see both Frank & Esper, 2005a and Büntgen *et al.*, 2008).

Nonhost data

Raw measurements of 2077 spruce (*Picea abies* Karst.) TRW series from 73 sites were considered as nonhost data (Fig. 1). Chronologies were processed in the same manner and divided into the same geographical sub-regions as performed for the host data. That is, division of the 73 spruce sites into six sub-regions resulted in regional nonhost time-series. These records comprised seven sites in the Southern Alps, 16 in the Western Alps, 24 in the Central Alps, eight (seven) in the lower (higher) Eastern Alps and 11 in the Tatra region. Earlier work showed the broad similarities in climate response of larch and spruce (Frank & Esper, 2005a), making this a suitable species to differentiate between climate- and insect-related variations. (See Büntgen *et al.* (2008) for details on growth trends and climate responses of the spruce data in this network.)

Outbreak detection

Six methods (i–vi) were applied to separate LBM (LBM, *Zeiraphera diniana* Gn.) outbreak-induced growth depressions from those caused by climatic or other biotic factors. The first three methods were performed on the basis of the individual measurement series at the tree level. These same methods were also applied to the mean site chronologies.

(i) Residuals between the individual larch host measurement series and the spruce nonhost chronologies, averaged over the corresponding geographical sub-region, were computed. The individual host and regional nonhost time-series were

scaled to means of 0.0 and standard deviations of 1.0, and each host series was subtracted from the corresponding nonhost chronology. The percentages of trees per site and year with negative residuals exceeding -1.5 were tabulated. For each site, years with $> 25\%$ of series affected were classified as outbreaks.

(ii) Each individual host series and the corresponding gridded temperature data were normalized (mean of zero, standard deviation of unity), and the host series was subtracted from the seasonal temperature mean with the highest correlation. Negative residuals exceeding -1.5 were considered to be indicative of an insect signal, with the percentage of trees per site per year used for LBM assessment. Years at each site with $> 25\%$ of affected series were regarded as outbreaks. It should be noted that the 18 host larch chronologies that did not reach sufficiently high correlations with any given temperature target were excluded from this routine.

(iii) A simple 15-yr moving window approach was used to identify extreme negative growth depressions probably associated with LBM outbreaks. In other words, a year at the centre of the moving window would be noted as a growth minimum if it had the lowest value with respect to the seven preceding and seven following years. For each year, the percentage of larch host series with identified minimum values was compiled. Those years having $> 25\%$ of series with local minima were regarded as outbreak candidates.

(iv–vi) The routines followed the same techniques as described above (i–iii), although residual analyses were performed on the larch host chronology level to overcome disturbances at the tree level – in each case, tree-ring data were de-trended using 20-yr cubic smoothing splines and, if utilized, temperature data were 20-yr high-pass filtered.

Although the first three techniques (i–iii) yielded continuous time-series of outbreak strength (intensity values exist for each year), the last three methods (iv–vi) yielded binary output (absence or presence values exist for each year). Outbreak intensity was classified into six levels, simply by summing the number of methods that detected an outbreak per site. Detection methods that were applied on the individual tree-level (i–iii) represent the classic epidemiological approach, whereby host individuals in a population were assessed and counted as being affected or not affected. By contrast, detection methods that were performed on the site-level (iv–vi) represent a mean value function assessment, indicating whether the sampled host site as a whole showed a sufficient signal to be identified as an outbreak. It is herein important to note that the potential underestimation of true outbreaks, which only affect a minority of individuals in a population, may emerge from using mean value functions. However, tree-by-tree assessments and counts possibly overestimate outbreaks that are less widespread within stands.

Our findings were compared with local evidence from the Swiss Lötschental (Esper *et al.*, 2007), the Italian Susa Valley (Nola *et al.*, 2006), the French Briançonnais (Rolland *et al.*,

2001) and sub-alpine discoloration maps (Baltensweiler & Rubli, 1999). In this regard, it should be noted that the thresholds of the six detection methods (i–vi) applied herein, even though various tests were performed, remain somewhat arbitrary. Wavelet analysis, following the techniques outlined in Torrence & Compo (1998), was applied to the reconstructed (AD 1700–2000) outbreak time-series from each site, the mean series from each of the five geographical sub-regions and the grand Alpine mean series. Moreover, the reconstructed insect outbreaks and seasonal temperature means were compared to evaluate potential climatic influences on both the detection methods applied and the LBM results obtained.

Three hundred and one annual maps of the greater Alpine region ($43\text{--}51^\circ\text{N}$ and $6\text{--}16^\circ\text{E}$) were generated to indicate intensity, spatial dispersal and temporal change in defoliation patterns back to AD 1700.

Results and Discussion

Outbreak occurrences

Periodic growth depressions caused by LBM outbreaks were not found in the TRW and MXD chronologies from the Tatra Mountains. These findings were consistent for the past three centuries and in general agreement with previous reports by Baltensweiler *et al.* (1977) and Büntgen *et al.* (2007). The absence of cyclic larch defoliation episodes most probably results from the restriction of larch to small and isolated stands along the Carpathian arc that do not provide adequate host material for the development of outbreaks. Given the absence of outbreaks in the Carpathians, further results and discussion are herein restricted to the Alpine arc only.

The detection of LBM outbreaks was classified at six different outbreak intensity levels, ranging from a minimum of one to a maximum of six positive detection methods. The sum of the number of positive detections (i–vi) averaged over all sites and the entire Alpine area provides evidence for 295 outbreaks during the interval AD 1700–2000 (Fig. 4). Only 6 yr were found without any defoliation signal [independent of the method (i–vi) applied]. Together, the six approaches revealed outbreak years during which 1.7–98.0% of the available sites were affected. By contrast, the outbreak intensity of the highest level, exclusively based on method (vi), was found in 110 yr. During these 110 cases, 1.5–24.0% of sites were affected (Fig. 4). There is an inherent compromise between detection being too sensitive (false positives) and not being sensitive enough (false negatives); the numbers of outbreaks detected decreased systematically with increasing numbers of detection methods used as a threshold (Figs 4, 5g). Lower outbreak intensity thresholds introduce background noise, whereas higher intensity thresholds restrict outbreak identification to more distinct peak events. [See also Swetnam *et al.* (1985) and Swetnam & Lynch (1993) for methodological implications of different thresholds used for the exposure of insect-induced

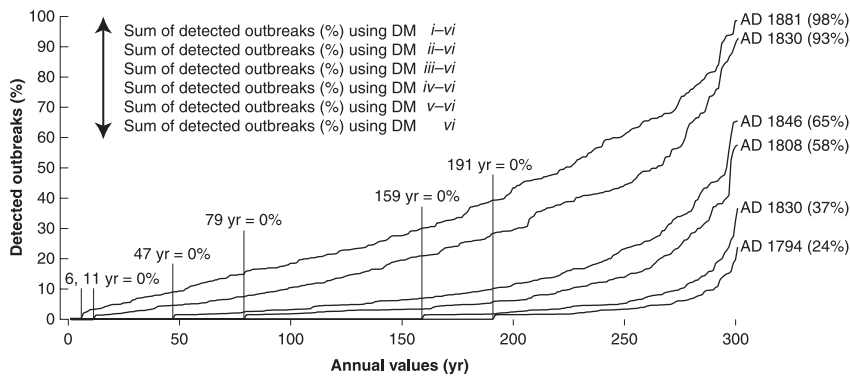


Fig. 4 Summary of the six (i–vi) detection methods (DM) applied. Black lines indicate the cumulative percentage of the detected outbreaks per year. The sum of all six methods (i–vi) shows outbreak evidence ranging from 1 to 98% in 295 yr, whereas 0% outbreak evidence is found in 6 yr, and the maximum of 98% outbreak evidence is reported for AD 1881. Maximum outbreak evidence, as defined by method (vi), reaches 24% in AD 1794, whereas 0% of evidence for this highest outbreak class (vi) is found for 191 yr between 1700 and 2000.

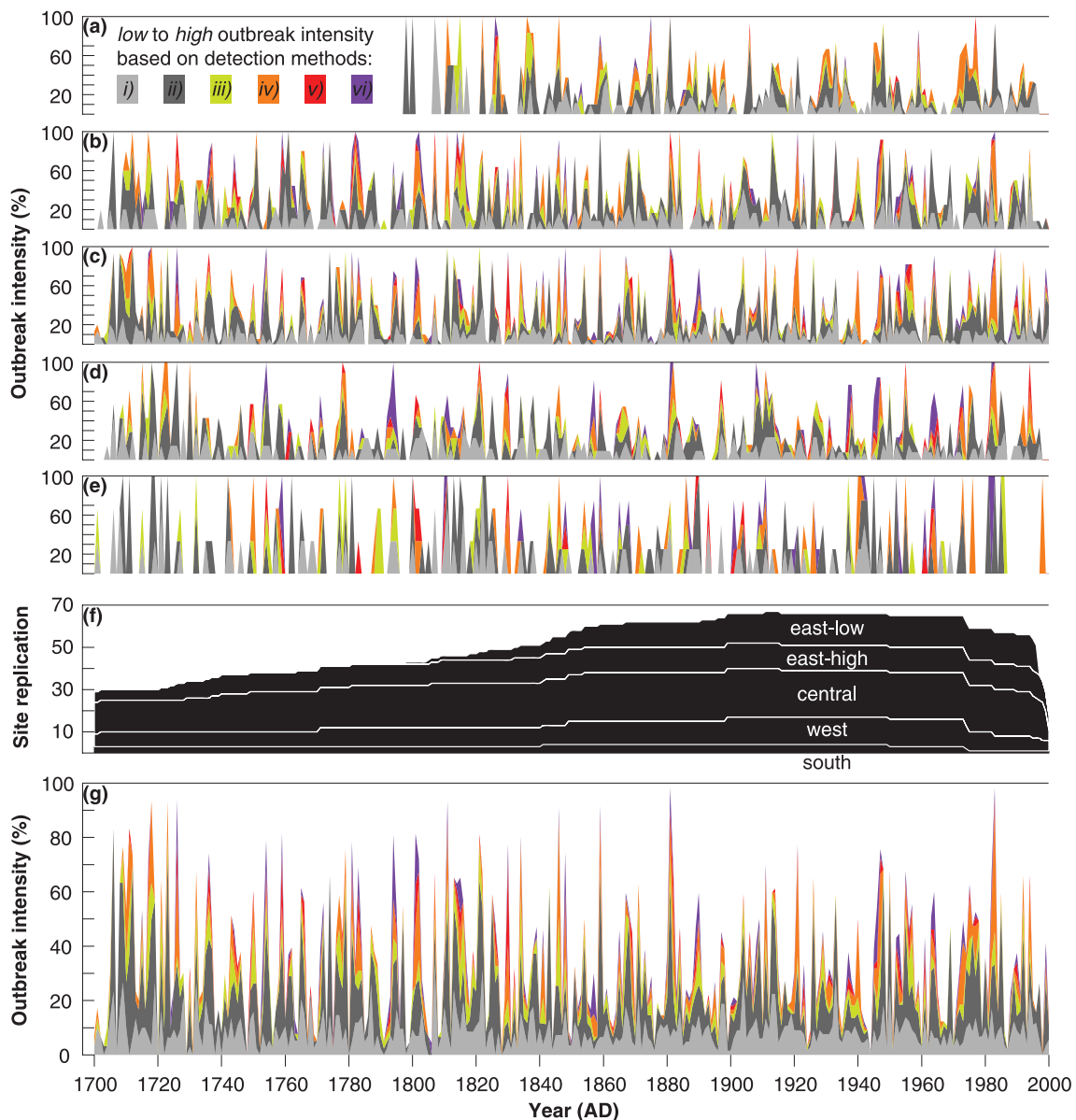
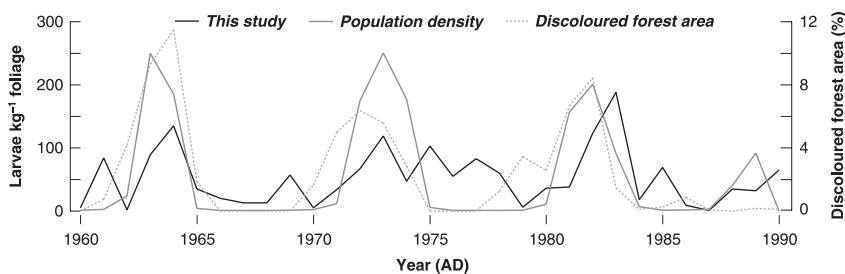


Fig. 5 Time-series of reconstructed larch budmoth (LBM) outbreaks (the cumulative percentage of the detected outbreaks per year following six intensity levels) over the 1700–2000 period and split into five geographical sub-regions: (a–e) south, west, central, east > 1500 and < 1500 m asl. (f) Site replication per sub-region and (g) outbreak patterns averaged over the entire Alpine arc. The six different colours refer to the six different outbreak intensities (ranging from low to high) that are based on the six detection methods (i–vi), as detailed in Fig. 4.

Fig. 6 Comparison between three cycles of reconstructed larch budmoth (LBM) outbreaks (this study), counted larvae population density and discoloured forest area (both from Baltensweiler & Rubli, 1999). Data are averaged over the entire Alpine arc and shown over their common period 1960–90.



disturbance signals in tree-ring chronologies.] The highest outbreak intensity (six of six methods were positive), which was obtained from > 10% of affected series per site, was limited to only 11 yr (1726, 1753–54, 1794, 1801, 1815, 1848, 1857, 1946, 1953 and 1964). Using a threshold of only one of six positive detections (one method of six revealed an outbreak), 15 events were detected in which > 80% of the available sites were affected (1706, 1711, 1718, 1723, 1726, 1759, 1794, 1801, 1811, 1821, 1834, 1846, 1859, 1881 and 1983).

The spatial characteristics of outbreaks can be inferred by observing patterns of outbreaks at sites grouped into five geographical sub-regions (Fig. 5a–e). The coincidence of several spikes in time-series is indicative of spatial synchrony, and the last well-synchronized population peak occurred between 1981 and 1983, exactly one century after the most severe Alpine outbreak in 1881. This last Alpine-wide outbreak event is even more distinct when averaging evidence from the five geographical sub-regions (Fig. 5g). Other well-synchronized 20th century outbreaks occurred in *c.* 1936, 1945, 1954, 1963, 1972 and 1981, with generally more asynchronous dynamics before and after this period. Supporting evidence for a decrease in population oscillation amplitude in the early 20th century has previously been presented across the Alps (Baltensweiler, 1993a; Baltensweiler & Rubli, 1999). The timing of local LBM outbreaks, quantified on the basis of larval counts and tree discoloration, generally matches peak populations estimated using tree-ring chronologies from the same locations (Rolland *et al.*, 2001; Nola *et al.*, 2006; Esper *et al.*, 2007). The detection of the seven most severe outbreak episodes identified here from the 20th century from the Southern and Western Alps is supported by Baltensweiler & Rubli (1999): 1908–09, 1935–37, 1945, 1953–54, 1962–63, 1971–72 and 1980–81. A detailed view on the three most prominent LBM outbreak cycles that spread across the Alpine arc, *i.e.* during the early 1960s, 1970s and 1980s, and considering independent evidence from tree ring-based outbreak reconstructions, survey-based larvae counts and observed forest discoloration, revealed temporal coherency (Fig. 6). It should be noted that such comprehensive information only exists for the mid-20th century. In addition, the existence of less significant local defoliation events during the early and mid-1990s is reported from all analyses, except Esper *et al.* (2007), who reconstructed outbreaks in a particular sub-alpine valley, although including data from different sites.

Wavelet analysis of the reconstructed (1700–2000) outbreak time-series, ranging from the site level to the grand Alpine mean, revealed insight into the persistence of defoliated cycles and their relationship to space. Figure 7 illustrates the obtained power spectra of highest intensity outbreaks (110 events during which all outbreak detection methods were positive), and low- to high-intensity outbreaks (295 events during which at least one of six methods was positive) averaged over the Alpine network. Evidence for significant power at a period of ~8 yr was greatest when using the highest outbreak level and diminished after the inclusion of lower outbreak intensities. Examination of the temporal variability in periodicity indicated a robust 8-yr period from ~1740 to 1820, at ~1850 and again from ~1930 to 1980 (Fig. 7a). The spectrum based on the lower intensity threshold was indicative of less distinct periodicity, with a significant shift of the global wavelet power towards a 32-yr period (Fig. 7b).

Wavelets using site-level LBM outbreak reconstructions are not shown herein; however, they supported the ‘altitude’ hypothesis, which postulates that the most severe LBM epidemics are concentrated at a range of elevations at ~1800 m asl (Weber, 1997). Site-specific spectra revealed a distinct periodicity at 8–9 yr from sites at elevations between 1750 and 1900 m asl (see Fig. 2 and Table S1 for the affected chronologies). Nevertheless, complex landscape geometries are likely to obscure both the direction and speed of travelling waves (Bjørnstad *et al.*, 2002; Johnson *et al.*, 2004, 2006), and local weather conditions may shift outbreak foci to lower or higher elevations and modulate populations at different slope exposures (Baltensweiler *et al.*, 2008). The assumption that optimal areas characterized by more frequent and intense outbreak amplitudes would consequently shift to higher elevations in a warming world becomes particularly critical in the long term, as the upper limit of most larch forests in the European Alps ranges between 1900 and 2100 m asl. Defoliation within lower elevation suboptimal zones may result from immigration from higher elevations (Baltensweiler & Rubli, 1999).

Climate interactions

Some caution should be exercised in interpreting these findings however, as it is possible that they are shaped by an altitudinal or spatial bias from uneven site replication throughout the

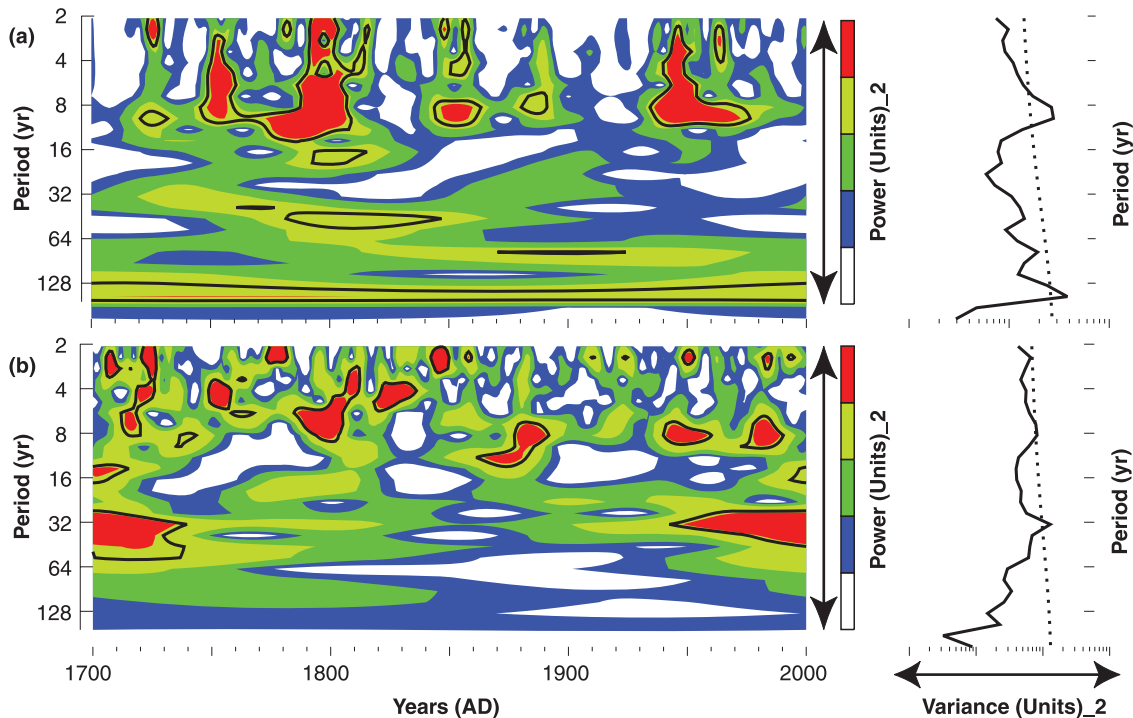


Fig. 7 Wavelet power spectra of Alpine-wide reconstructed outbreak time-series based on: (a) 110 events during which detection method (vi) (all routines were positive) indicated an outbreak for 1.5–24.0% of affected site chronologies, and (b) 295 events during which the sum of the six detection methods indicated an outbreak for 1.7–98.0% of affected site chronologies. Contour levels are chosen so that 75, 50, 25 and 5% of the wavelet power is above each level, respectively. Black contour is the 10% significance level, using a white-noise background spectrum. Right side shows the corresponding global wavelet power spectra (black line). Broken lines denote significance, assuming the same significance level and background spectrum as indicated above.

five geographical sub-regions – ranging from four sites in the Southern Alps to 23 sites in the Central Alps (see Fig. 5f for details on sample size). The few high-intensity outbreaks reconstructed from the low-elevation cluster (Fig. 5a) simply result from the fact that only four of the 15 sites could realistically be compared with climate data. The remaining low-elevation chronologies that did not correlate at $r \geq 0.25$ with temperature (see Fig. 3 for details) consequently were unable to yield reconstructed outbreaks of higher intensity (see Materials and Methods section above). Methodological caution is further advised because the running minima approach may interpret any negative growth extreme as an artificial defoliation event. In this regard, it should be noted that a combination of the six outbreak detection methods (i–vi) most probably represents the best tool to distinguish annual growth depressions caused by LBM from other disturbance factors, such as climate anomalies or more local disturbances caused by logging, rock fall and lightning that are quite common at higher elevations.

Reconstructed defoliation was not perfectly synchronized across the entire Alpine arc, and this indicates a lack of significant climate forcing on the detection method(s) applied. That is, cyclic outbreak episodes obtained via negative growth anomalies mismatch any particular temperature regime that occurred across the Alps. There often is a danger of circular

reasoning in tree ring-based reconstructions of insect defoliation (Kress *et al.*, 2009), which has been detailed for the western spruce budworm in the USA (Ryerson *et al.*, 2003). For example, negative growth anomalies may result from below average summer temperatures, but spuriously be interpreted as population outbreaks. Overlapping temperature depressions and insect defoliation are thus difficult to distinguish, although the applied nonhost comparison probably reduced this risk. Increases in growing season temperatures, which are known to stimulate TRW and MXD at the upper timberline, would yield positive growth anomalies (Büntgen *et al.*, 2005, 2006b; Frank & Esper, 2005a,b), subsequently compensating for defoliation-induced growth interruptions (Baltensweiler *et al.*, 2008). The possibility of climate-driven cycles in population dynamics is unlikely, given that regular ~8–10-yr oscillations have not been reported from climatic observations. Various methodological tests on the detection of outbreak-induced growth depressions in tree-ring data have been conducted in the northern USA using host spruce budworm (Swetnam *et al.*, 1985; Morin *et al.*, 1993; Swetnam & Lynch, 1993; Ryerson *et al.*, 2003) and pandora moth data (Speer *et al.*, 2001). All of these studies stressed the importance of clearly separated climatic and ecological information (Arabas *et al.*, 2008). Moreover, a tendency for increasing error back in time might derive from: (1) a general reduction in sample size at

the site level; (2) an overall decline in site chronology at the network level; (3) a less homogeneous spatial site distribution across the network; and (4) a more insecure temperature record during the 17th and 18th centuries (Frank *et al.*, 2007a), and particularly before *c.* 1760 when documentary evidence dominated (Casty *et al.*, 2005).

The assessment of seasonally resolved Alpine temperature variability denoted the last two decades to be a period during which temperatures in all seasons were well above the 20th century mean. This warming parallels the disappearance of LBM outbreaks in a 1200-yr cyclic reconstruction from the Swiss Alps (Esper *et al.*, 2007), and a severe dampening in synchronized Alpine-wide defoliation (Baltensweiler, 1993a). At the same time, fading population cycles in voles and grouse have been associated with global warming (Ims *et al.*, 2008). The recognition of drifting in and out cyclic dynamics could, to some extent, be data and methodologically driven, and thus be prematurely linked to climatic warming (Parmesan, 2007). By contrast, the widespread and simultaneous absence of high-amplitude cyclic population densities cannot be related to local and methodological factors only. Uncertainty in our understanding of potential oscillation dampening since about the 1980s interestingly derives from a period of reduced data availability (Fig. 2b) (see Frank *et al.*, 2007a for a discussion). Evidence for the weakening of the LBM oscillations derives from exhaustive survey data that are lacking into the late 20th century (Baltensweiler & Rubli, 1999), and a spatially constrained study in the Swiss sub-alpine Lötschental (Esper *et al.*, 2007).

Physiological aspects

Both TRW and MXD include valuable information necessary for defoliation reconstruction; TRW contains a higher degree of biological memory, whereas MXD is characterized by less autocorrelation and recovers faster from any disturbance (Esper *et al.*, 2007; Frank *et al.*, 2007a). Mean lag-1 autocorrelation of the Alpine TRW site chronologies utilized herein is 0.53, with generally higher values deriving from higher elevation sites, and overall lower values being reported for MXD (see Table S1 for site-specific information). Carry-over effects that mainly bias earlywood cell formation (Fritts, 1976) can yield towards a slight delay of detected extremes (Fig. 6). This is related to integrative effects from previous year climatic and ecological conditions on TRW formation, which can be further obscured by longer term gain (loss) in activating resources from root and needle growth following favourable (severe) conditions (Frank *et al.*, 2007a). Only the consequent coexistence of both TRW and MXD measurements allows defoliation-induced vs climate-induced persistence in cell development and enlargement to be distinguished (Esper *et al.*, 2007).

Additional insights on abiotic forcing may also originate from stable $\delta^{13}\text{C}$ - and $\delta^{18}\text{O}$ -isotope ratios, which have recently

been reported to be less prone to insect defoliation (Kress *et al.*, 2009). Negligible effects of LBM outbreaks on stable isotopic ratios indicate that defoliation is independent of changes in leaf physiology, known to modulate carbon and oxygen values (Leavitt & Long, 1988). Rather than reflecting changes in stomatal conductance and photosynthetic capacity, $\delta^{18}\text{O}$ composition of cellulose may be shifted towards the isotopic signature of source water, as little leaf water enrichment occurs during defoliation. The synchronous behaviour of both carbon and oxygen isotopes during LBM defoliation events partly supports the hypothesis that isotope composition is climate controlled (Kress *et al.*, 2009). During outbreak years, tree-ring cellulose is formed either before the devastating feeding occurs or shortly thereafter, when host trees re-foliate roughly 1 month after defoliation (Baltensweiler *et al.*, 2008). The timing of late summer re-foliation, which theoretically could account for a positive relationship between summer warmth and LBM outbreaks, has been assessed recently (Kress *et al.*, 2009). Such a relationship would also reflect the previously postulated effect of cold season temperatures on LBM diapause and, subsequently, population growth (Baltensweiler, 1993b). The development of first-stage larvae in spring is limited by the energy provided at the time of oviposition in the previous summer. Optimal conditions for first instars are long and cold winters with more than 120 d below 2°C (Baltensweiler, 1993b). If summer temperatures are high, development from egg to moth is terminated sooner, leading to an earlier diapause with fewer frost days, resulting in an elevated egg mortality plus increased larval mortality when hatching before host needle flushing (Baltensweiler *et al.*, 1977). In addition, larch foliage quality for various larval stages has been implicated to play a central role in population oscillations (Baltensweiler, 1993b). As a result of the yearly re-growth of needles, LBM larvae depend on needle maturation and have to cope with large changes in food quality (e.g. raw fibre and protein content). Seasonal synchronization of larval development with needle maturation is a requirement for population growth and outbreak development (Asshoff & Hattenschwiler, 2006). Even a slight temporal offset between larval and foliar development may have serious consequences on LBM population growth. Warmer summer temperatures may also affect the relative timing of LBM and its parasitoids, with implicit effects on population dynamics.

Several different mechanisms have been suggested to explain LBM oscillations, such as behavioural changes in population quality (Baltensweiler, 1993a), insect–disease interactions (Anderson & May, 1980), induced host defences (Fischlin, 1982) and host–parasitoid dependences (Turchin *et al.*, 2003). As discussed above, there are many possible mechanisms by which climate may alter LBM dynamics, but there remains considerable uncertainty with regard to how populations are modulated by climate change (Esper *et al.*, 2007). We point out parenthetically that no indication of thermal effects on outbreak intensity and periodicity was evident for the 1940s,

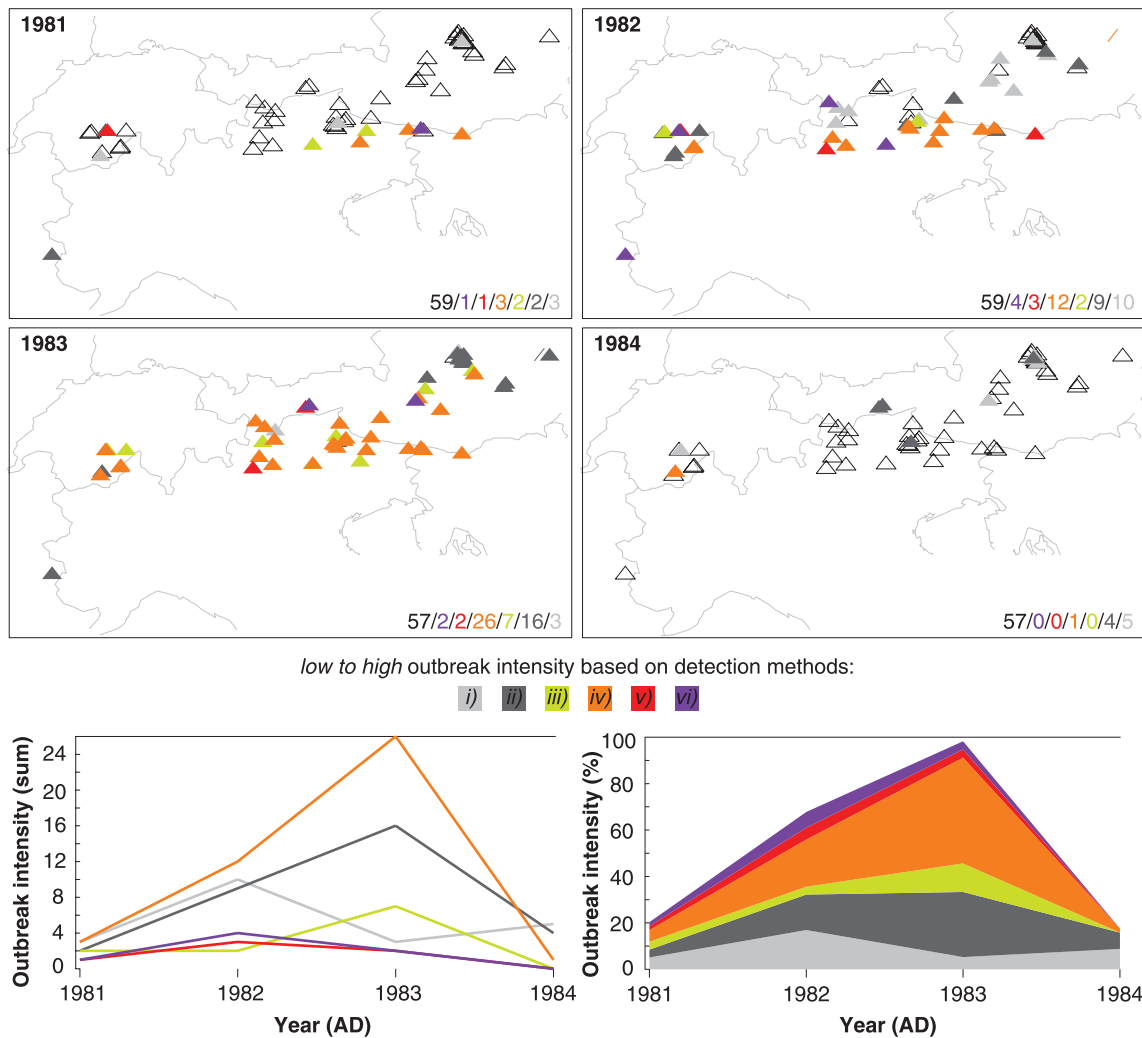


Fig. 8 Annually resolved maps of the last Alpine-wide synchronized larch budmoth (LBM) outbreak event during 1981–84. Thin black triangles show the existing site chronologies per year, and colours refer to the reconstructed outbreak intensity ranging from heavy (purple) to low (grey). The six different colours are based on the six detection methods (i–vi), as detailed in Fig. 4. The corresponding numbers at the bottom right of the figures summarize each year's data availability and outbreak intensity, with the bottom graphs describing these numbers (outbreak sum per intensity level and cumulative percentage of the intensity levels) over time. Annual maps for 1700–2000 are provided in Fig. S1 (see Supporting Information).

a decade during which spring and summer temperatures were comparable with those of the late 20th century (Auer *et al.*, 2007). By contrast, early 20th century winter temperatures were much cooler than during recent times, even though considering some degree of bias inherent to early instrumental station measurements (Frank *et al.*, 2007a). Unprecedented high temperatures amongst all seasons are a unique feature of the past two decades only.

Spatial patterns

We provide 301 maps that describe annual patterns of Alpine-wide LBM outbreak dispersal (Fig. S1a–i, see Supporting Information). A total of 29 site chronologies is available in

1700, and replication ranges from 18 sites in 2000 to 67 sites between 1911 and 1915. The number of LBM outbreaks per year ranges from 0% (in 6 yr) to 98% (in AD 1881). Figure 8 summarizes the spatial and temporal aspects of the last Alpine-wide outbreak that occurred in the early 1980s. Although four maps illustrate the distribution and intensity of the defoliated sites per year, the chronological evolution from 1981 to 1984 is further highlighted by the simple sum or cumulative percentage of the positive cases derived from the six detection methods (i–vi). Considering the full 1700–2000 period of evidence, distinct periodicity is reconstructed for the mid-18th century, the transition from the 18th to 19th century and again for the mid-20th century. Less intense and/or spatially less synchronized outbreaks appeared at the transition from

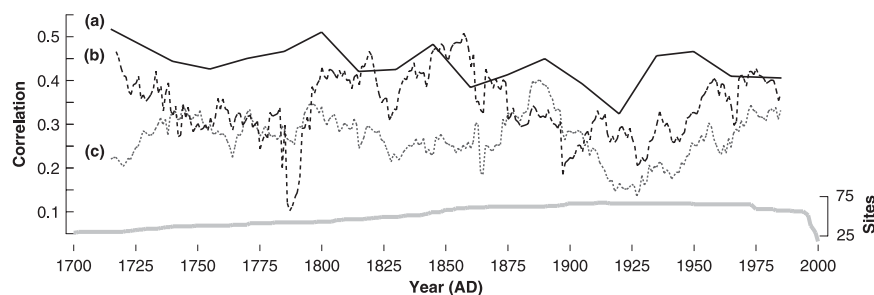


Fig. 9 Moving correlation analysis computed between: (a) 70 larch budmoth (LBM) outbreak reconstructions of the site-level (full line), (b) between five LBM outbreak reconstructions of the geographical sub-regions (black broken line), and (c) between six LBM outbreak reconstructions of different intensity levels (grey broken line). Correlations are computed over 30-yr windows and lagged by 15 yr along the individual site records (a), and continuously shifted by 1 yr along the time-series of the geographical sub-regions (b), and those of the different intensity levels (c). Site replication over the full 1700–2000 period is indicated by the bottom solid grey line.

the 19th to 20th century. Moving correlation analysis computed between the 70 reconstructed LBM outbreak time-series of the site level provides some indication for temporal changes in outbreak synchrony across the Alpine arc and over the 1700–2000 period (Fig. 9a). Strongest agreement is found during the early 18th century, ~1800, ~1840 and during the mid-20th century. Lowest correlations are obtained in the early 20th century. Similar correlation analysis using the five reconstructed LBM outbreak time-series that represent the geographical sub-regions (Fig. 9b), or using the six records that reflect the different outbreak intensity levels [following detection methods (i–vi)] (Fig. 9c), show similar changes in synchrony over time. Caution, however, is advised during the calculation's start and end periods, where site replication is low. Moreover, the spatial data coverage of our network merely reflects sampling activities of the various data contributors rather than an even geographical and altitudinal distribution. Site location was weighted towards the western Swiss Alps, two centres in the Italian Alps and one lower elevation cluster in the Eastern Austrian Alps. To obtain a more uniform distribution of samples, more data would be needed from the south-west French and Italian Alps, along the entire northern pre-Alps, some parts of the Central Alps and from higher elevations in Austria and generally lower elevations everywhere else.

Conclusions and perspective

We compiled TRW and MXD measurement series from 70 larch host and 73 spruce nonhost sites distributed across the European Alps and Tatra Mountains spanning elevations from 500 to 2300 m asl. This unique network integrates living trees from six countries and historical wood from the Swiss Alps. The sample size is robust, i.e. allows spatial patterns to be analysed for more than three centuries.

Six LBM outbreak detection methods were applied to distinguish negative growth depressions caused by insect defoliation from depressions caused by climatic, ecological or other biotic factors. The first three methods were performed on the basis of the individual measurement series, whereas the

remaining methods were applied on the mean site chronologies. These include the calculation of residuals between host (larch) and nonhost (spruce and climate) surrogates, and running minima analysis. The outbreak events obtained were classified into six intensity levels. Comparison with seasonal temperature means was performed to evaluate potential climatic influences on both the detection methods applied and reconstructed LBM outbreaks. For the first time, annual maps of reconstructed LBM outbreak intensity were developed for the Alpine arc dating back to AD 1700.

These reconstructions indicated the existence of synchronized 20th century outbreak pulses at *c.* 1936, 1945, 1954, 1963, 1972 and 1981, with generally more spatial heterogeneity being characteristic before and after this period. Robust 8-yr cycles were detected at *c.* ~1740–1820, ~1850 and again from ~1930 to 1980. Wavelet spectra based on site-level reconstructed outbreak series indicate distinct periodicity at 8–9 yr for sites in the Western Alps between 1750 and 1900 m asl. The combination of six methods sufficiently distinguished between annual growth depressions caused by LBM and other disturbance factors, such as climate anomalies. Seasonally resolved Alpine temperature variations indicated long-term warming during winter, spring and autumn, but stationary summer temperatures over the past three centuries. Unprecedented warming in all seasons characterized the post-1980 period. Distinct outbreak periodicity is mapped for the first decades of the 18th century, the transition from the 18th to 19th century and again from the mid-20th century until the early 1980s. Less intense and/or spatially less synchronized outbreaks appeared during the mid-18th century, the transition from the 19th to 20th century and during the recent warming. Local persistence, but spatial heterogeneity, in cyclic population dynamics is characteristic for the Alpine arc during the past three centuries. However, more data and revised methodologies are necessary to enhance the estimates of long-term outbreak dynamics.

Based on these results, we suggest that future research on the LBM system should investigate: (1) altitudinal dependence in outbreak intensity, timing, phase angle and climate forcing;

(2) relationships between tree growth and needle length as the main food supply, with particular emphasis on effects of host quality on cycle occurrence and spatial dispersal; (3) parameter-specific, i.e. TRW, MXD, defoliation responses at differing site locations and ecology; (4) outbreak effects on tree-ring isotopes; and (5) improved separation between insect- and climate-induced fingerprints via model simulations. Increasing awareness and collaboration between biologists, ecologists and climatologists will improve our understanding of responses in population dynamics and forest communities to climate variability and change. Moreover, mutual attention in assessing the linkage between (internal) responses of ecosystems and (external) climate forcing is an impetus for launching interdisciplinary research.

Acknowledgements

M. Schmidhalter, M. Seifert and various ITRDB (International Tree Ring Data Bank; <http://www.ncdc.noaa.gov/paleo/treering.html>) contributors provided tree-ring measurements. C. Casty made the climate data available. K. Treydte and D. Schmatz established the ALP-IMP (#01.0498-1) databank, and M. Carrer was supported by the University of Padova project EXTRA (CPDA071953). Three anonymous reviewers added valuable comments on an earlier version of the manuscript. Funded by the European Union project MILLENNIUM (#017008-GOCE) and the SNSF (Swiss National Science Foundation) project EURO-TRANS (#200021-105663).

References

- Anderson RM, May RM. 1980. Infection, diseases and population cycles of forest insects. *Science* 210: 658–661.
- Arabas KB, Black B, Lentile L, Speer J, Sparks J. 2008. Disturbance history of a mixed conifer stand in central Idaho, USA. *Tree-Ring Research* 64: 67–80.
- Asshoff R, Hattenschwiler S. 2006. Changes in needle quality and larch bud moth performance in response to CO₂ enrichment and defoliation of treeline larches. *Ecological Entomology* 31: 84–90.
- Auer I, Böhm R, Jurkovic A, Lipa W, Orlik A, Potzmann R, Schöner W, Ungersböck M, Matulla C, Briffa K *et al.* 2007. HISTALP – Historical instrumental climatological surface time series of the Greater Alpine Region. *International Journal of Climatology* 27: 17–46.
- Baltensweiler W. 1993a. Why the larch bud moth cycle collapsed in the subalpine larch-cembraan pine forests in the year 1990 for the first time since 1850. *Oecologia* 94: 62–66.
- Baltensweiler W. 1993b. A contribution to the explanation of the larch bud moth cycle, the polymorphic fitness hypothesis. *Oecologia* 93: 251–255.
- Baltensweiler W, Benz G, Bovey P, Delucchi V. 1977. Dynamics of larch bud moth populations. *Annual Reviews on Entomology* 22: 79–100.
- Baltensweiler W, Rubli D. 1999. Dispersal – an important driving force of the cyclic population dynamics of the larch bud moth. *Forest Snow and Landscape Research* 74: 3–153.
- Baltensweiler W, Weber UM, Cherubini P. 2008. Tracing the influence of larch-bud-moth insect outbreaks and weather conditions on larch tree-ring growth in Engadine (Switzerland). *Oikos* 117: 161–172.
- Berryman AA. 1996. What causes population cycles of forest Lepidoptera? *Trends in Ecology and Evolution* 11: 28–32.
- Bjørnstad ON, Peltonen M, Liebhold AM, Baltensweiler W. 2002. Waves of larch budmoth outbreaks in the European Alps. *Science* 298: 1020–1023.
- Böhm R, Auer I, Brunetti M, Maugeri M, Nanni T, Schöner W. 2001. Regional temperature variability in the European Alps: 1760–1998 from homogenized instrumental time series. *International Journal of Climatology* 21: 1779–1801.
- Büntgen U, Bellwald I, Kalbermatten H, Schmidhalter M, Freund H, Frank DC, Bellwald W, Neuwirth B, Nüsser M, Esper J. 2006a. 700 years of settlement and building history in the Lötschental/Switzerland. *Erdkunde* 60: 96–112.
- Büntgen U, Esper J, Frank DC, Nicolussi K, Schmidhalter M. 2005. A 1052-yr tree-ring proxy for Alpine summer temperatures. *Climate Dynamics* 25: 141–153.
- Büntgen U, Frank DC, Kaczka RJ, Verstege A, Zwijacz-Kozica T, Esper J. 2007. Growth/climate response of a multi-species tree-ring network in the Western Carpathian Tatra Mountains, Poland and Slovakia. *Tree Physiology* 27: 689–702.
- Büntgen U, Frank DC, Nievergelt D, Esper J. 2006b. Summer temperature variations in the European Alps, AD 755–2004. *Journal of Climate* 19: 5606–5623.
- Büntgen U, Frank DC, Wilson R, Carrer M, Urbinati C, Esper J. 2008. Testing for tree-ring divergence in the European Alps. *Global Change Biology* 14: 2433–2453.
- Casty C, Wanner H, Luterbacher J, Esper J, Böhm R. 2005. Temperature and precipitation variability in the European Alps since 1500. *International Journal of Climatology* 25: 1855–1880.
- Cook ER, Peters K. 1981. The smoothing spline: a new approach to standardizing forest interior tree-ring width series for dendroclimatic studies. *Tree-Ring Bulletin* 41: 45–53.
- Cook ER, Peters K. 1997. Calculating unbiased tree-ring indices for the study of climatic and environmental change. *The Holocene* 7: 361–370.
- Esper J, Büntgen U, Frank DC, Nievergelt D, Liebhold A. 2007. 1200 years of regular outbreaks in alpine insects. *Proceedings of the Royal Society B* 274: 671–679.
- Fischlin A. 1982. *Analyse eines Wald-Insekten-Systems: Der Subalpine Lärchen-Arvenwald und der Graue Lärchenwickler Zeiraphera diniana Gn. (Lepidoptera, Tortricidae)*. Dissertation Number 6977. Zurich, Switzerland: ETH Zürich.
- Fischlin A, Baltensweiler W. 1979. Systems analysis of the larch bud moth system: the larch–larch bud moth relationship. *Mitteilungen der Schweizerischen Entomologischen Gesellschaft* 52: 273–289.
- Frank D, Esper J. 2005a. Characterization and climate response patterns of a high elevation, multi species tree-ring network for the European Alps. *Dendrochronologia* 22: 107–121.
- Frank D, Esper J. 2005b. Temperature reconstructions and comparisons with instrumental data from a tree-ring network for the European Alps. *International Journal of Climatology* 25: 1437–1454.
- Frank D, Esper J, Cook E. 2007b. Adjustment for proxy number and coherence in a large-scale temperature reconstruction. *Geophysical Research Letters* 34: doi: 10.1029/2007GL030571, 1–5.
- Frank DC, Büntgen U, Böhm R, Maugeri M, Esper J. 2007a. Warmer early instrumental measurements versus colder reconstructed temperatures: shooting at a moving target. *Quaternary Science Reviews* 26: 3298–3310.
- Fritts HC. 1976. *Tree rings and climate*. London, UK: Academic Press.
- Ims RA, Henden J, Killengreen ST. 2008. Collapsing population cycles. *Trends in Ecology and Evolution* 23: 79–86.
- Johnson DM, Bjørnstad ON, Liebhold AM. 2004. Landscape geometry and traveling waves in the larch budmoth. *Ecological Letters* 7: 967–974.
- Johnson DM, Bjørnstad ON, Liebhold AM. 2006. Landscape mosaic induces traveling waves of insect outbreaks. *Oecologia* 148: 51–60.
- Kendall BE, Prendergast J, Bjørnstad ON. 1998. The macroecology of population dynamics: taxonomic and biogeographic patterns in population cycles. *Ecology Letters* 1: 160–164.

- Kress A, Saurer M, Büntgen U, Treydte K, Bugmann H, Siegwolf R. 2009. Summer temperature dependency of larch budmoth outbreaks revealed by Alpine tree-ring isotope chronologies. *Oecologia*, doi:10.1007/s00442-009-1290-4
- Leavitt SW, Long A. 1988. Stable carbon isotope chronologies from trees in the southwestern United States. *Global Biogeochemical Cycles* 2: 189–198.
- Liebhold A, Kamata N. 2000. Are population cycles and spatial synchrony a universal characteristic of forest insect populations? *Population Ecology* 42: 205–209.
- Lindström ER, Hörnfeld B. 1994. Vole cycles, snow depth and fox predation. *Oikos* 70: 156–160.
- Mitchell TD, Jones PD. 2005. An improved method of constructing a database of monthly climate observations and associated high-resolution grids. *International Journal of Climatology* 25: 693–712.
- Morin H, Laprise D, Bergeron Y. 1993. Chronology of spruce budworm outbreaks near Lake Duparquet, Abitibi region, Quebec. *Canadian Journal of Forest Research* 23: 1497–1506.
- Myers JH. 1988. Can a general hypothesis explain population cycles of forest lepidoptera. *Advances in Ecological Research* 18: 179–242.
- Nola P, Morales M, Motta R, Villalba R. 2006. The role of larch budmoth (*Zeiraphera dimiana* GN.) on forest succession in a larch (*Larix decidua* Mill.) and Swiss stone pine (*Pinus cembra* L.) stand in the Susa Valley (Piedmont, Italy). *Trees Structure and Function* 20: 371–382.
- Parmesan C. 2006. Ecological and evolutionary responses to recent climate change. *Annual Reviews of Ecology, Evolution and Systematics* 37: 637–669.
- Parmesan C. 2007. Influences of species, latitudes and methodologies on estimates of phenological responses to global warming. *Global Change Biology* 13: 1860–1872.
- Rolland C, Baltensweiler W, Petitcolas V. 2001. The potential for using *Larix decidua* ring widths in reconstructions of larch budmoth (*Zeiraphera dimiana*) outbreak history: dendrochronological estimates compared with insect surveys. *Trees, Structure and Function* 15: 414–424.
- Ryerson D, Swetnam TW, Lynch AM. 2003. Tree-ring reconstruction of western spruce budworm outbreaks in the San Juan Mountains of Colorado. *Canadian Journal of Forest Research* 33: 1010–1028.
- Schweingruber FH. 1979. Auswirkungen des Lärchenwicklerbefalls auf die Jahrringstruktur der Lärche. *Schweizerische Zeitschrift für Forstwesen* 130: 1071–1093.
- Speer JH, Swetnam TW, Wickman BE, Youngblood A. 2001. Changes in pandora moth outbreak dynamics during the past 622 years. *Ecology* 82: 679–697.
- Steen H, Ims RA, Sonerud GA. 1996. Spatial and temporal patterns of small-rodent population dynamics at a regional scale. *Ecology* 77: 2365–2372.
- Stenseth NC. 1999. Population cycles in voles and lemmings: density dependence and phase dependence in a stochastic world. *Oikos* 87: 427–461.
- Stenseth NC, Mysterud A, Ottersen G, Hurrell JW, Chan K, Lima M. 2002. Ecological effects of climate fluctuations. *Science* 297: 1292–1296.
- Swetnam TW, Lynch AM. 1993. Multi-century, regional-scale patterns of western spruce budworm history. *Ecological Monographs* 63: 399–424.
- Swetnam TW, Thompson MA, Sutherland EK. 1985. Using dendrochronology to measure radial growth of defoliated trees. *USDA Forest Service, Agriculture Handbook* 639: 39.
- Torrence C, Compo GP. 1998. A practical guide to wavelet analysis. *Bulletin of the American Meteorological Society* 79: 61–78.
- Turchin P, Wood SN, Ellner SP, Kendall BE, Murdoch WW, Fischlin A, Casas J, McCauley E, Briggs CJ. 2003. Dynamical effects of plant quality and parasitism on population cycles of larch budmoth. *Ecology* 84: 1207–1214.
- Weber U. 1997. Dendrochronological reconstruction and interpretation of larch budmoth (*Zeiraphera dimiana*) outbreaks in two central alpine valleys of Switzerland from 1470–1990. *Trees Structure and Function* 11: 277–290.
- Wigley T, Briffa KR, Jones PD. 1984. On the average of value of correlated time series, with applications in dendroclimatology and hydrometeorology. *Journal of Climatology and Applied Meteorology* 23: 201–213.

Supporting Information

Additional supporting information may be found in the online version of this article.

Fig. S1 (a–i) Annually resolved maps of Alpine-wide larch budmoth (LBM) outbreaks of the period 1700–2000.

Table S1 Characteristics of the 70 larch sites sorted by elevation, and statistics referring to 300-yr spline chronologies

Please note: Wiley-Blackwell are not responsible for the content or functionality of any supporting information supplied by the authors. Any queries (other than missing material) should be directed to the *New Phytologist* Central Office.